Predictive Modelling of Osmotic Dehydration of Food Materials

Duduyemi Oladejo, Oluoti K.O, Adedeji K.A., Raji N.A.

Abstract— **During osmotic dehydration of food materials, water and/or other substances are removed from the material with molecular infiltration; shrinkage follows depending on the extent of net mass loss. Molecular diffusion is one of the generally accepted and necessary tools for finding simple predictive models that describe mass transfer across plant membranes. The mass transfer resistances across a semi-permeable medium were investigated with Fickian molecular diffusion model and a combined molecular and convective model. The effects of intercellular and trans-membrane resistances studied with two-parameter kinetic models described the behaviours of solute impregnation and dewatering processes of osmotic dehydration. Predicted depth of solute impregnation in an imaginary food matrix was 4.0 mm with satisfactory deduction that combined molecular and convective model is a better description of the transport models. The solutions of the models also revealed that concentration gradient across the membranes depends linearly on process variables and the influences of membranous resistance were not negligible**

Index Terms— **Diffusion, Inter membranous resistances, Impregnation, Osmotic dehydration.**

I. INTRODUCTION

Mass transfer is usually predicted through modelling. However, common models developed for osmotic dehydration of fruits and vegetables make assumptions that often deviate far from reality, including large heterogeneity, variability and complexity in properties of fruits and vegetables. Mathematical models based on mass transfer across plant membranes are important tools in finding simple predictive models that could be used to describe the concepts of osmotic dehydration in food processing. Fick's second law is generally accepted for modelling mass transfer operations by diffusion during osmotic dehydration [1].

Two basis of explanation of diffusion reported in literature were investigated based on the assumptions that internal resistances to mass transfer was negligible hence, the effect of convective mass transfer resulting from concentration gradient alone results in linear dependency on process variables [2]. The second approach is the two-parameter kinetic model consisting of intercellular and trans-membrane transport which are configured to offer significant resistances

Duduyemi Oladejo, Department Of Chemical And Polymer Engineering, Lagos State University, Epe Campus Lagos, Nigeria.
Oluoti K.O, Department Of Chemical And Polymer Engineering, Lagos State University, Epe Campus Lagos, Nigeria.
Adedeji K.A., Department Mechanical Engineering Lagos State University, Epe Campus Lagos, Nigeria.
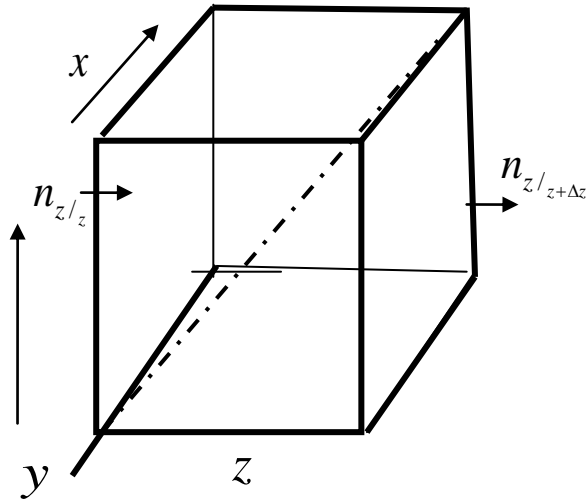**Raji N.A.,** Department Mechanical Engineering Lagos State University, Epe Campus Lagos, Nigeria.

to impregnation dewatering (osmotic dehydration) processes [3].

The premise is based on the influence of inter-cellular and intra-membrane resistances to mass transport, but also taking into account the mass exchange across the cell membrane between inter-cellular and intra-membrane resistances. The mass transport within inter-cellular and intra-membrane osmotic dehydration paths include diffusion of solute within the media and potential gradient due to concentration differences that is responsible for hydrostatic pressure gradient, whereas across the cell membrane, it includes both osmotic and ultra-filtration flow [4].

Some researchers consider that solute penetration occurs in extracellular spaces since these compartments are only partially selective and there is always some solute diffusion into the food [5]. Other workers suggest that water loss is greater than solute gain primarily because of differences between the diffusion coefficient of water and that of solute in the product [6]. Consequently, the diffusion coefficient, which is expected to be constant exhibits diverse values depending on the operating parameters and media of interest. Hence, lists of diffusion coefficient relationships for different media were proposed [7]**.** Each of the relationships needs to be tested to find the most suitable diffusivity coefficient for evaluating the extent of OD in a particular system.

Therefore, it is imperative to model the change in concentration with respect to convective and bulk mass transfers during solute and water transport across food cellular membrane and the osmotic solution. These developed and solved models would be employed in predicting the trends of OD with respect to the time of immersion, chemical potentials due to concentration gradient and the extent of solute impregnation at specified boundary conditions.

II. THEORETICAL CONSIDERATION

Using an elemental balance approach for a cubic volume of imaginary food structure of unit thickness to represent the fruit or vegetable matrix as illustrated in Figure 1. The law of conservation of mass was applied to the control volume and its effect on the rate of mass transport is described in equation 1.0 [8]:

$$\frac{\partial m_{(in)}}{\partial t} + \frac{\partial m_{(out0}}{\partial t} + \frac{\partial m_{(genrated)}}{\partial t} = \frac{dM_{acc}}{dt}$$

1.0

where M is the total accumulated mass and '*m*' represents the mass in transit.

Figure 1: Elemental volume representation of a unit mass of the material matrix.

A. 2.1 Convective Transport Model for Osmotic Dehydration

Assumptions:

To develop the model considering both molecular and convective mass transport, the following assumptions are necessary:

i.   No reaction occurs between the osmotic solution and the food constituents;

ii. The molecules of cell organelles and nutrients remain non-diffusing outside the cell due to inter-molecular and intra-membrane resistances;

iii. Only sugar and water molecules migrate between the food material and the osmotic solution;

iv. The solutes and water are perfectly miscible without precipitation.

v.   The process is isothermal;

Therefore in mathematical terms, overall mass transfer, equation 1.0 can be expressed in the form of law of conservation of materials:

$$\sum Input - \sum Output + \sum Generated = \sum Accumulation$$

(2.0)

Applying simplifying assumptions to component material balance across a unit portion of material in the *x*, *y*, and *z* planes yields equation 3

$$(n_x|_x - n_x|_{x+\Delta x})\Delta y\Delta z + (n_y|_y - n_y|_{y+\Delta y})\Delta x\Delta z + (n_z|_z - n_z|_{z+\Delta z})\Delta y\Delta x = \frac{\partial \rho}{\partial t}\Delta x\Delta y\Delta z$$

(3)

Mass velocity per unit volume $n = \rho v$, where ρ= density and v = velocity

If the flow in the y and z directions is negligible, then flow in the x-direction is shown in equation 3.0:

$$(n_x|_x - n_x|_{x+\Delta x})\Delta y\Delta z = \frac{\partial \rho}{\partial t}\Delta x\Delta y\Delta z$$

(4.0)

Dividing both sides of equation 4 by, $\Delta x\Delta y\Delta z$ gives: 5:

$$\frac{n_x|_x - n_x|_{x+\Delta x}}{\Delta x} = \frac{\partial \rho}{\partial t}$$ (5)

Taking the limits as $\Delta x \rightarrow \partial x$:

$$-\frac{\partial n_x}{\partial x} = \frac{\partial \rho}{\partial t}$$ (6)

The mass flow rate, 'n_x' can be expressed in terms of the fluid density as product of number of moles and molecular mass. Therefore, a differential mass flow rate along the x-axis is substituted to obtain equation 7:

$$-\frac{\partial(MN)}{\partial x} = \frac{\partial \rho}{\partial t}$$ (7)

where *MN* = Summation of both diffusion and convective flux. Hence, they are inter-dependent and non-linear. Since no bulk motion occurs in the system because of the internal and external resistances, equation 7 becomes:

$$MN = MJ$$ (8)

The total mass transferred (flux) is equivalent to molecular transport 'J' defined by Fick's first law:

$$J = -\frac{D\partial C}{\partial x}$$ (9)

Therefore, substituting equations 8 and 9 into equation 7:

$$-\frac{\partial}{\partial x}\left[M\left(-\frac{D\partial C}{\partial x}\right)\right] = \frac{\partial \rho}{\partial t}$$ (10)

Rearranging, and noting that ρ is directly proportional to concentration, one obtains equation 3.20 [9, 10]:

$$\frac{\partial C}{\partial t} = \frac{D\partial^2 C}{\partial x^2}$$ (11)

Equation 11 is the unsteady state Fickian's 2nd law of diffusion model.

B. 2.2 Explicit Finite Difference Equation

The (RHS) of equation 11 by finite difference gives equation 12:

$$\frac{\partial C}{\partial t} = \frac{C_{i,j}^{n+1} - C_{i,j}^n}{\Delta t}$$ (12)

The second order finite difference of equation 12 yields equation 13:

$$\frac{\partial^2 C}{\partial x^2} = \frac{C_{i+1,j}^n - 2C_{i,j}^n + C_{i-1,j}^n}{\Delta x^2}$$ (13)

Substituting equations 12 and 13 into equation 10 gives:

$$\frac{C_{i,j}^{n+1} - C_{i,j}}{\frac{\partial \rho}{\partial t}\Delta x\Delta y\Delta z} = D\left[\frac{C_{i+1}^n - 2C_{i,j} + C_{i-1,j}^n}{\Delta x^2}\right]$$ (14)

Arranging equation 14 in terms of concentration difference, yields equation 15:

$$C_{i,j}^{n+1} - C_{i,j}^n = \frac{D\Delta t}{\Delta x^2}\left[C_{i+1,j}^n - 2C_{i,j} + C_{i-1,j}\right]$$ (15)

Define $A=D\Delta t/\Delta z$, where *D* represents the diffusion coefficient.

Using the Wilke-Chang expression of diffusivity correlations for binary mixtures [2]. The Diffusivity constant is defined:

$$D_{AB}^0 = \frac{7.4 \times 10^{-8}(\phi_B M_B)^{1/2} T}{\mu_B V_A^{0.6}}$$ (16)

where M_B = molecular weight =of water 18.016 g/mol

$$\phi_B = \text{Association factor} = 2.26$$

$$T = Temperature = 298K; \quad room \ temperature$$

$$\mu_B = vis\cos isty \ \text{of solvent} = 9.5 \times 10^{-4} \ Pas.$$

$$V_A = \text{molar volume of solute at normal boiling point} = 1.0134 \times 10^6 \ g/m^3$$

Solving equation 15 by stepwise iteration yields equation 17:

$$C_{i,j}^{n+1} = C_{i,j}^n + AC_{i+2,j}^n - 2AC_{i,j}^n + AC_{i-1,j}^n$$
(17)

Collecting like terms and re-arranging:

$$C_{i,j}^{n+1} = (1-2A)C_{i,j}^n + AC_{i+1,j}^n + AC_{i-1,j}^n \qquad (18)$$

Equation 18 is the finite difference (explicit) model showing the stepwise concentration variation with respect to the time of immersion, and the extent of solute impregnation or penetration.

C. 2.3 Solution to the Model Equations

The initial and boundary conditions based on the range of experimental values of concentration variations in the literature are:

Initial conditions:

At time, t = 0, concentration, C= 60 °Bx, and at time t > 0; sucrose concentration (°Bx).

Boundary conditions:

At x = 0, C = 60 °Bx

$x = X$ =20 mm, C = 60 °Bx

Δx = step of iteration along X

Time t ranges from 0 to 105 min, step of iteration Δt = 5 min Diffusivity D = constant from Wilke-Chang expression of diffusivity (cm²/s)

At infinite time, the concentration of sugar in the fruit is assumed similar to that in the solution, hence, dehydration process would be at equilibrium and the media become isotonic. The simulation of the model equation with MATLAB 2007 explains the concentration profile in the medium as a function of both time and the depth of penetration using defined initial and boundary conditions.

D. 2.4 Kinetic Model for Molecular and Convective Mass Transport

The model was developed on the following additional assumptions:

i. The molecular transport depended mainly on diffusion while the convective transport was dependent on osmotic pressure imposed by concentration gradient.

ii. There was no resistance at the surfaces; and

iii. Sugar solution films exist as a boundary layer with selective permeability thus allowing for trans-membrane transport at isothermal condition.

Applying these assumptions to the continuity equation from first principle in the x-direction, equation 18 so derived is upgraded. Convert the mass flux to concentration gradient by dividing both sides of equation (7) by molar mass (Mm) to define the osmotic solution concentration, would yield equation 19:

$$-\frac{1}{Mm}\frac{\partial n_x}{\partial x} = \frac{1}{Mm}\frac{\partial p}{\partial t} \qquad 19$$

where N_x is molar flux, and C_A is the solute concentration gave equation 20:

$$-\frac{\partial N_x}{\partial x} = \frac{\partial C_A}{\partial t} \qquad 20$$

Structural parameters such as sample volume, specific dimensions and porosity were closely related to mass transfer processes [11]. Therefore introducing the constitutive equation of Fick's law of diffusion to the molecular transport of solute and solvent gives equation 21:

$$N_x = -D_{AB}\frac{\partial C_A}{\partial x} + C_A V_M \qquad (21)$$

where diffusion due to molecular transfer is represented by $\{-D_{AB}\frac{\partial C_A}{\partial x}\}$, while the term $C_A V_M$ is diffusion due to convective transfer (bulk fluid). N_x is molar flux, D_{AB} is diffusivity, V_M is molar average velocity.

To determine the extent of molecular penetration $\frac{\partial N_x}{\partial x}$, differentiate both sides of the equation 3.30 with respect to x and open the bracket to obtain equation 22:

$$\frac{\partial N_x}{\partial x} = \frac{\partial}{\partial x}(-D_{AB}\frac{\partial C_A}{\partial x}) + \frac{\partial}{\partial x}(C_A V_M) \qquad 23$$

Therefore, simplifying further yields equation 24:

$$\frac{\partial N_x}{\partial x} = -D_{AB}\frac{\partial^2 C_A}{\partial x^2} + \frac{\partial}{\partial x}(C_A V_M) \qquad (24)$$

Substituting equation 24 into equation 20, gives equation 25:

$$D_{AB}\frac{\partial^2 C}{\partial x^2} - \frac{\partial}{\partial x}(C_A V_M) = \frac{\partial C_A}{\partial t} \qquad (25)$$

Expanding $C_A V_M$; the diffusion due to convective transfer (bulk fluid) in equation 24:

$$\frac{\partial}{\partial x}(C_A V_M) = V_M\frac{\partial C_A}{\partial x} + C_A\frac{\partial V_M}{\partial x} \qquad (26)$$

Therefore substituting equations 25 into 26 gives the time dependent concentration profile equation 27:

$$D_A \frac{\partial^2 C_A}{\partial x^2} - (V_M \frac{\partial C_A}{\partial x} + C_A \frac{\partial V_M}{\partial x}) = \frac{\partial C_A}{\partial t}$$

(27)

Equation 27 is the model equation describing concentration profile in an osmotically dehydrated product as a function of time of immersion, the extent of penetration which primarily depends on the food structure and the concentration of the osmo-active agents.

E. 2.5 Explicit Finite Difference Model For The Combined Mass Transport Equation

Removing the bracket in equation 27 yields equation 28:

$$D_{AB} \frac{\partial^2 C_A}{\partial x^2} - V_M \frac{\partial C_A}{\partial x} - C_A \frac{\partial V_M}{\partial x} = \frac{\partial C_A}{\partial t} \qquad (28)$$

Introducing finite difference solution approach, to simplify equation 28 leads to equation 29:

$$D_{AB}\left(\frac{C_{A_{i+i,j}} - 2C_{A_{i,j}} + C_{A_{i-1,j}}}{\Delta x^2}\right) - V_M\left(\frac{C_{A_{i+1,j}} C_{A_{i-1,j}}}{2\Delta x}\right) - kC_{A_{i,j}} = \left(\frac{C_{A_{i,j+1}} - C_{A_{i,.}}}{\Delta t}\right)$$

(29)

where

$$k = \frac{\partial V_M}{\partial x} = \text{constant}$$

Expanding equation 29 and rearranging it as a function of transient concentration yields equation 30:

$$C_{A_{i+1,j}}\left(D_{AB}\frac{\Delta t}{\Delta x^2} - V_M\frac{\Delta t}{2\Delta x}\right) + C_{A_{i,j}}\left(1 - k\Delta t - \frac{2D_{AB}\Delta t}{\Delta x^2}\right) + \Delta t C_{A_{i-1,j}}\left(\frac{D_{AB}}{\Delta x^2} + \frac{V_M}{2\Delta x}\right) = C_{A_{i,j+1}}$$

$$Let\ A = \frac{\Delta t}{\Delta x^2}\left(D_{AB} \overset{....(31)}{-} V_M\right)$$

$$B = 1 - k\Delta t - \frac{2D_{AB}\Delta t}{\Delta x^2}$$

and

$$D = \left(\frac{D_{AB}}{\Delta x^2} + \frac{V_M}{2\Delta x}\right)\Delta t$$

Therefore, equation 31 can be arranged into a linear expression represented by equation 32:

$$AC_{A_{i+1,j}} + BC_{A_{i,j}} + DC_{A_{i-1,j}} = C_{A_{i,j+1}} \qquad (32)$$

Equation 32 is the finite difference model, a representation of combined molecular and convective mass transport within and around an imaginative sample of material osmotically treated.

III. SOLUTION APPROACH TO THE TRANSPORT MODEL DERIVED

Flow across the boundary was assumed to agree to Dirichlet conditions, as it describes the medium appropriately having constant boundary values of variables at any given time. The parabolic partial differential equation (P.D.E) with initial value problem (IVP) approach was considered [12]:

(i) Initial Value Condition
$$C(X_o, t) = 0.0\ ^oBx$$
$$for\ t=0,\ X_o = X$$

(ii) Boundary Value Condition
$$C(X_o, t) = 60\ ^oBx \text{ - an assumed liquid}$$
concentration of sucrose based on the upper limits used in practical applications elsewhere [13].

$$for\ t>0,\ X_o = 0$$
$$C(X,t) = 60\ ^0Bx$$
for t ≥ 0, X=L

where C represents concentration as a functions of extent of penetration distance X for a given time 't', L represents the length of the sample while subscript 'o' signifies the initial set point.

These initial and boundary conditions were applied to solve the model equations (18) and (3.38) on MATLAB (2007) simulink to explain the kinetics of osmotic dehydration with respect to the inter-cellular and intra-membranous resistances to mass transport. The 3-D plots were also generated. The response of the structural resistances as defined by initial and boundary conditions were studied one after the other. Each mathematical model was simulated with MATLAB 2007 (7.5) to generate predictive analysis of the dependent variables. An algorithm for the solution is presented.

3.1 The Algorithm For The Simulation Of Derived Explicit Finite Difference Model

1) Define the initial functions.
2) Input the Data: Diffusivity coefficient, molar velocity time of simulation, initial and final concentration of solute, the number of x and t sub-intervals.
3) Compute dx, dt and the coefficients of the equation.
4) Clear header table and print the first line.
5) Dimension the arrays to grid size.
6) Initialize concentration variables.
7) Set-counter and a repetitive structure for the number of grid size..
8) Compute concentrations for all the grid points.
9) Print result for concentration with corresponding points on the matrix and simulation time.
10) Continue loop until the last grid point, then stop.
11) Plot the concentration profile for the solute concentration with space and time.
13) End program.

IV. RESULTS AND DISCUSSIONS

4.1 Prediction of the Kinetic Model Equation

Model equations 18 and 31 derived for both convective and combined molecular and convective mass transport systems were solved to obtain the concentration profiles in finite imaginary samples. Both equations demonstrated that the rate of dehydration and impregnation was exponential in nature and similar to the model in the form of equation 4.5 [14, 15].

$$\ln\left(C/C_0\right) = \ln(k) + n\ln(t) \qquad (5)$$

where: C_o and C are respectively, the initial and final concentrations; t is time; k is the kinetic rate constant and n is a dimensionless coefficient.

Model equations derived from the Fickian law was solved numerically and simulated using Matlab programs to explain effects of the process variables from the plots.

4.2 THE CONVECTIVE OSMOTIC DEHYDRATION MODEL

The solution to the convective osmotic dehydration model equation 18 gave the simulation data presented in Table 1. The trend of concentration profile established during the OD process showed a marked decrease in concentration of the processing liquor from 60 to about 58.8 °Bx as shown in

Figure 2. The plot also revealed that effective osmotic dehydration time is less than 120 min. The extent of solute impregnation (depth of penetration) with respect to time is presented in the 3D plot Figure. 3. The plot showed that solute penetration was linearly degraded around the matrix of the imaginary sample because of the potential difference between osmotic solution and the sample. It also suggests that the rate of solute impregnation may not be the same as the rate of osmotic dehydration. In the convective OD model, where resistance to mass transfer was assumed negligible concentrations are higher in the extracellular volume than in the intracellular volume. Hence, the diffusion coefficients assumed in the extracellular volume are generally higher than those assumed for the intracellular volume [4]

ABLE 1.0: Simulated Concentration Data as Functions Depth of Penetration and Time.

Time (min)	Depth of penetration (mm)					
	3	6	9	12	15	18
0.0	0.0500	0.0500	0.0500	0.0500	0.0500	0.0500
5	0.6000	0.0500	0.0500	0.0500	0.0500	0.0500
15	0.6000	0.0622	0.0500	0.0500	0.0500	0.0500
20	0.6000	0.0739	0.0503	0.0500	0.0500	0.0500
25	0.6000	0.0851	0.0508	0.0500	0.0500	0.0500
30	0.6000	0.0957	0.0515	0.0500	0.0500	0.0500
35	0.6000	0.1060	0.0525	0.0501	0.0500	0.0500
40	0.6000	0.1158	0.0536	0.0501	0.0500	0.0500
45	0.6000	0.1251	0.0549	0.0502	0.0500	0.0500
50	0.6000	0.1341	0.0564	0.0503	0.0500	0.0500
55	0.6000	0.1428	0.0580	0.0504	0.0500	0.0500
60	0.6000	0.1510	0.0597	0.0506	0.0500	0.0500
65	0.6000	0.1590	0.0615	0.0508	0.0500	0.0500
70	0.6000	0.1666	0.0634	0.0510	0.0500	0.0500
75	0.6000	0.1740	0.0655	0.0512	0.0501	0.0500
80	0.6000	0.1810	0.0676	0.0515	0.0501	0.0500
85	0.6000	0.1878	0.0697	0.0519	0.0501	0.0500
90	0.6000	0.1943	0.0719	0.0522	0.0502	0.0500
95	0.6000	0.2006	0.0742	0.0526	0.0502	0.0500
100	0.6000	0.2067	0.0766	0.0530	0.0503	0.0500
105	0.6000	0.2125	0.0789	0.0535	0.0503	0.0500
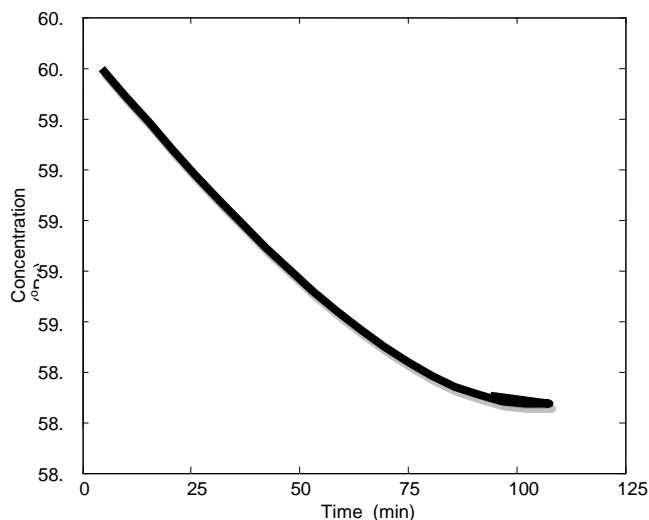
Figure 2: Concentration Vs Time Profile of Solute Impregnation across the Imaginary Sample.
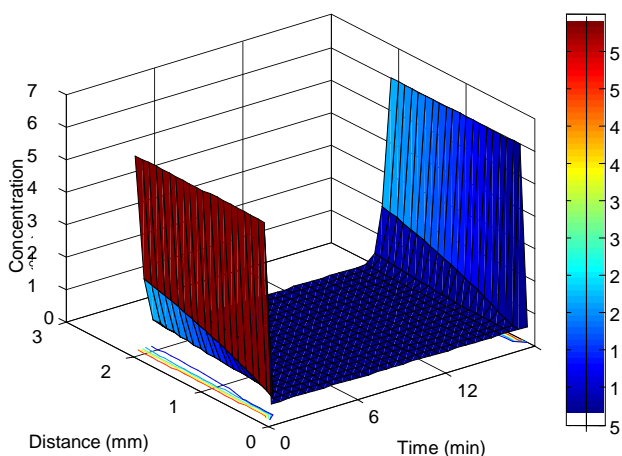
Figure 3: The Convective Mass Transport Model across a Finite Imaginary Sample
(NB: Colour legend bar indicating the concentration variations around the imaginary sample).

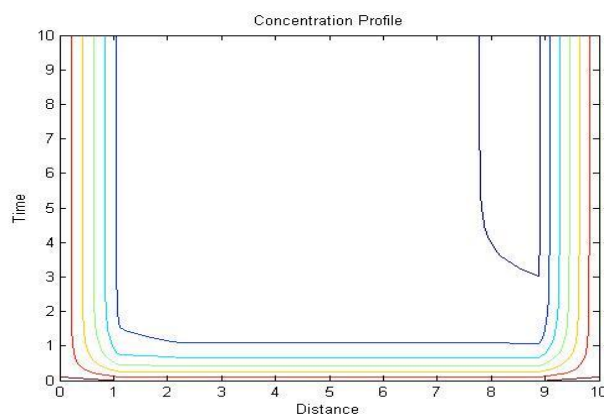### 4.3 Combined Molecular and Convective Transport Model

When sample was immersed in concentrated osmotic solution, solutes in the solution start to diffuse into the sample through both intracellular and extracellular spaces The solution to the model equation (31) as simulated with MATLAB 7.5 program codes generated the spatial 3-D plot as functions of sucrose concentration around an imaginary sample, time and depth of penetration (solute impregnation) using the defined boundary conditions. The contour plots from the simulation showing combined transient responses of imaginary samples to osmo-impregnation soaking of the dehydration system to changes in concentration, time and depth of solute impregnation is shown in Figure 4.

The 3D plot exhibited the profiles of solute impregnation and concentrations around the imaginary sample for the combined molecular and convective mass transport It provided a description of the modified distance pattern of solute impregnation, which was observed to be non-linear around the sample boundaries. It demonstrated the rapid clogging of sample surfaces at the very early stages of the process thus limiting the extent of solute impregnation and restricting mass

transfer across the membrane. The process was rapid at the beginning and gradually decreased to a stationary point near the surface while the inner matrices were seemingly unaffected. Therefore, the assumption that external resistance to mass transfer is negligible may not be entirely valid [16].

The structure of solute concentration across an imaginary sample is shown in the distance dependent plot Figure 5. It describes the pattern of solute penetration during the first 120 min. The plot revealed that effective depth of solute penetration was less than 4-mm into the sample matrix. This result was in agreement with the conclusion of reported experimental study of osmotic dehydration of Chestnut slab to the effect that penetration of sucrose after 4hr was only important for sample zone less than 4mm near the surface [13]. Therefore, the structural characteristics of the sample would be affected at the exterior nature of each sample. On the other hand, the transverse appraisal of the transport model (kinetics) across the imaginary sample is simulated (Figure 6). There was a drastic reduction in the transfer rate of solute from the solution into the sample after the attainment of saturation at the periphery to the depth of about 3 mm. This can be interpreted on the basis of higher water mass transfer coefficients (k_w) occurrence which prevailed at the outer boundaries of the sample for a short while leading to hindered mass transfer. This would suggest that there existed an external resistance to mass transport of the solute into and to water removal out of the sample which would be in consonance with previous findings by [2]. It demonstrated that internal features of the sample were not affected. However, the upsurge of solute increase at one extreme end suggested that major dehydration occurred at the periphery of the imaginary sample.

One implication of these simulation results could be that solute concentration did not have a tangible effect in some parts of the sample and that solute impregnation only occurred at the periphery up to a depth of less than 4.0 mm. This possibility lends credence to a phenomenon reported for carrot in earlier studies [16, 1]. Hence, during osmotic dehydration, the possibility may exist that a superficial layer of solute less than 4-mm deep is formed on the sample surface in the nature of a boundary layer. Thus, intercellular and intra-membrane resistances could have a major negative effect on mass transfer, favouring water loss while limiting solute deposition and reducing the loss of water-soluble solutes [17].

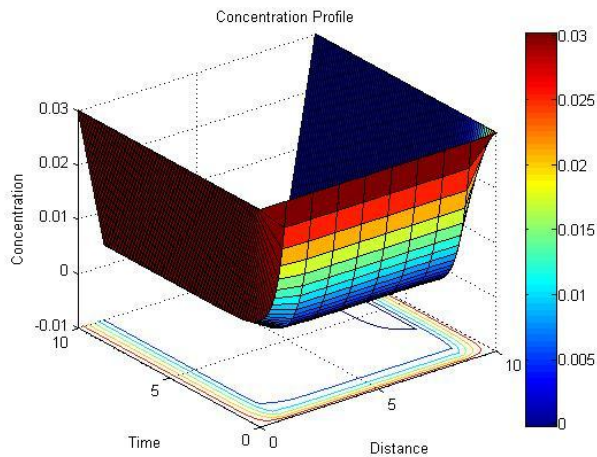Figure 4: Concentration Profile Contour Plots in Imaginary Sample

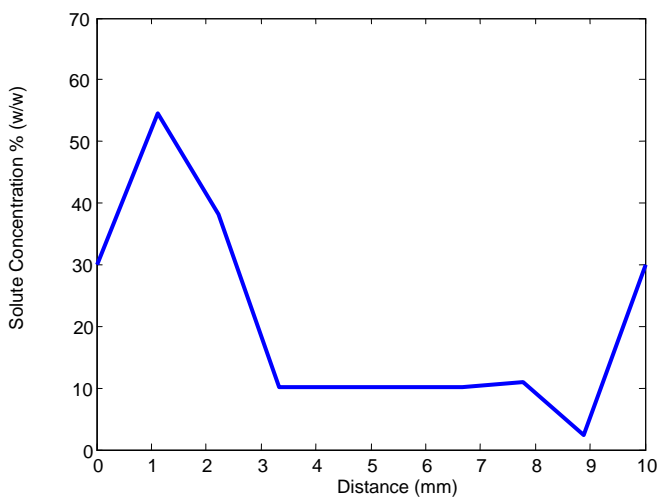Figure 5: The Combined Molecular and Convective Mass Transport Model

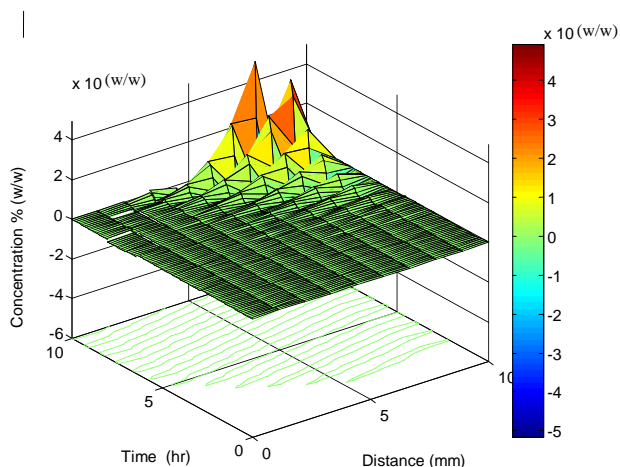Figure 6: Distance dependent simulation of solute concentration across imaginary sample

Figure 7: Concentration profile in-out simulation across imaginary sample matrix

Consequently, if further dehydration is desired, it would require the imposition of additional chemical potential which would explain why OD cannot produce a shelf-stable product but can only serve as a pre-treatment step to further processing in achieving more robust preservation in long-term storage. Deductively, the extent of dehydration can be said to depend more importantly on the residence time of immersion, while dehydration rate would depend on differential osmotic pressure. Slight differences in concentration profiles of the two models Figures 3 and 4 are attributable to postulated resistances induced by concentration gradients, thus showing the respective effects of molecular and convective mass transfer kinetics.

Solutes would find its way across the intracellular and extracellular spaces on the basis of the assumptions of negligible resistance. In contrast, the combined effects of molecular and convective forces induced higher resistances in the path of dehydration. Increase in solute concentration across the sample would therefore imply that solute infusion from the solution into the surrounding intercellular spaces would, in turn, have a corresponding increase in the matrix solute concentration resulting in enhanced osmotic pressure with time. Consequently, the kinetic model, which propounded combined molecular and convective effects, provided a better description of the osmotic dehydration process. These theoretically deductive arguments have sought to provide plausible elucidations of new process behaviour and mechanism. The effects of trans-membrane and intercellular resistances during osmotic transport were affirmed to be relevant at the commencement of the dehydration process. However, as soon as impregnation-soaking phenomenon advanced to the 4-mm point, the overall resistance imposed an equilibrium which rendered further dehydration almost impossible.

V. CONCLUSIONS

Mathematical models based on mass transfer kinetics in an imaginary sample were developed to describe the osmotic dehydration process. The models confirmed that a combination of molecular and convective mass transfer mechanisms was more effective in representing the influence of intercellular and intra-membranous resistance on osmotic dehydration especially for descriptive non-linear, modified distance mode of impregnation. The depth of solute penetration was estimated to be less than 4.0 mm. The effect of solute concentration on peripheral water loss and solute gain were not linear but exponential as predicted by the models investigated. The models developed can be used to predict the results of osmotic dehydration under any stated conditions of sucrose concentration, temperature, and processing residence time.

REFERENCE

[1] Rastogi, N.K. and Raghavarao, K.S.M.S. (2004). Mass transfer during osmotic dehydration of pineapple considering Fickian diffusion in cubical configuration, Lebensmittel-Wissenschaft und-Technologie, (37): 43–47.

[2] Tonon A., Renata V., Alessandra F. Baroni b, Mı´riam D. Hubinger (2007). Osmotic dehydration of tomato in ternary solutions: Influence of process variables on mass transfer kinetics and an evaluation of the retention of carotenoids. Journal of Food Engineering 82 509–517

[3] Piotr P.L. and Andrzej L. (2007). Experimental data on osmotic dehydration of cylindrical shaped carrot samples. Osmotic Dehydration of Fruits and Vegetables . pp 763-854

[4] Long-yuan Li (2006). Numerical simulation of mass transfer during the osmotic dehydration of biological tissues. Computational Materials Science. 35:75–83

[5] Matusek A. and Merész P. (2002). Modeling of sugar transfer during osmotic dehydration of carrots.. Periodica Polytechnica Series Chemical Engineering, 46, (1): 83–92.

[6] Sereno, A.M.; Moreira, R.; Martinez, E. (2001). Mass transfer coefficients during osmotic dehydration of apple in single and combined aqueous solutions of sugar and salt. Journal of Food Engineering, 47: 43.

[7] Perry R.H. and Don W.C. (1999). Perry's Chemical Engineers' Handbook. Seventh Edition, Macgraw Hill incorporation.

[8] Joseph P.R., John S.J. and Louis T.(2002). Handbook of Chemical and Environmental

[9] Engineering calculations. A John Wiley and Sons, Inc., Publication. Canada.

[10] Rastogi N.K., Raghavarao K.S.M.S., Niranjan K. and Knorr D. (2002). Recent developments in osmotic dehydration: methods to enhance mass transfer. Trends in Food Science and Technology 13: 48–59.

[11] Azuara, Cortes, Garcia and Bristain, 1992 Azuara, E., Cortes, R., Garcia, H.S., and Bristain, C.I. (1992). Kinetic model for osmotic dehydration and its relationship with Fick's second law. International Journal of Food Science and Technology, 27: 409–418.

[12] Barat *et al*., 2001 Barat, J.M, Fitto P. and Chiralt A. (2001). Modeling of simultaneous mass transfer and structural changes in fruits tissues. Journal of Food Engineering, 49: 77-85.

[13] Norman W.L. (2007) Applied Mathematical Methods for Chemical Engineers. Second Edition, CRC Press Boca Raton.

[14] Chenlo, R. Moreira, C. Ferna´ndez-Herrero, G. Va´zquez (2007). Osmotic dehydration of chestnut with sucrose: Mass transfer processes and global kinetics modelling. Journal of Food Engineering 78:765–774.

[15] Ade-Omowaye, B. I. O (2002). Application of Pulsed Electric fields as a pre-treatment step in the Processing of plant based foods. 1st Edition Cuvillier Verrlag Publisher Berlin.

[16] Shivbare, U.S., Guptar M., Basu S. and Raghavan (2006). Kinetics of Osmotic Concentration of Carrot Preserve. Journal of Food Technology 4(3):200-205,

[17] Marcotte and Le Maguer, 1992 and Marcotte, M., LeMaguer, M., 1991, Repartition of water in plant tissues subjected to osmotic processes, Journal of Food Process Engineering, 13(4), pp. 297-320

[18] Azarpazhooh, E. and Ramaswamy, H.S. (2010). Osmotic Dehydration, in Drying of Foods, Vegetables and Fruits - Volume 1, Ed. Jangam, S.V., Law, C.L. and Mujumdar, A.S., ISBN - 978-981-08-6759-1, Singapore.